JACS
JOURNAL OF THE AMERICAN CHEMICAL SOCIETY
pubs.acs.org/JACS
Communication

Supramolecular Alternating Donor–Acceptor Assembly toward Intercalated Covalent Organic Frameworks

Huiqing Li, Pengpeng Shao, Shuqi Chen, Guosheng Li, Xiao Feng, Xiong Chen, Hui-Jun Zhang,* Jianbin Lin,* and Yun-Bao Jiang

Cite This: J. Am. Chem. Soc. 2020, 142, 3712–3717
Read Online
ACCESS | Metrics & More | Article Recommendations | Supporting Information

ABSTRACT: Conventionally, *z*-direction modulation of two-dimensional covalent organic frameworks (2D-COFs) is difficult to achieve because they rely on spontaneous $\pi-\pi$ interactions to form 3D architectures. Herein, we report a facile construction of a novel intercalated covalent organic framework (Intercalated-COF) by synchronizing operations of supramolecular donor–acceptor (D–A) interactions (A unit: 2,5,8,11-tetra(*p*-formylphenyl)-perylene diimide (PDI) **1**; D unit: perylene **3**, as intercalator) in the vertical directions, with polymerizations (by only reacting **1** with *p*-phenylenediamine **2**) in the lateral directions. In this Intercalated-COF, the PDI-based covalent 2D layers are uniformly separated by perylene guest layers. This supramolecular strategy opens the possibility for *z*-direction modulation of 2D-COFs through "intercalating" various guest molecules and thus may contribute to the exploration of advanced applications of these porous and crystalline frameworks.

Exploring advanced applications of new materials relies on exquisite utilization of their structure uniqueness and facile manipulations of the architectures. In recent years, two-dimensional covalent organic frameworks (2D-COFs)[1] have attracted considerable scientific interest for their potential applications in catalysis,[2] gas storage/separation,[3] solid state batteries,[4] sensing,[5] and optoelectronics, as well as photovoltaics.[6] In general, 2D-COF synthesis is dominated by both lateral growth of covalent-bonded single-layers and vertical extension of the frameworks through less controllable π-stacking of the 2D-layers.[7] Until now, the exploration of 2D-COFs predominantly relied on the modulation of size, symmetry, and linkage of building blocks, which can precisely define the topology, composition, and ordering in the covalent 2D layers. In contrast, despite the significance of π-stacking in the formation, stability, and property-modulation of 2D COFs,[8] only a few principles have been proposed to improve or alter the vertical stacking behaviors of the repeated 2D layers.[9] In this context, with proper supramolecular assembly systems, specific guest molecules could be "intercalated" between the covalent layers of normal COF structures through a bottom-up approach, leading to novel intercalated COFs (Intercalated-COFs) with *z*-direction controllable layered heterostructures (Scheme 1). This approach is inspired by the structural regulation mode of graphite to graphite intercalation compounds (GICs) and could in turn be developed into a brand-new field of research.[10] More importantly, distinct to GICs, Intercalated-COFs provide a unique opportunity to be constructed with diversified building blocks.

As one special case of π-stacking, columnar alternating aromatic donor–acceptor (D–A) stacking has been successfully used in the construction of a wide variety of supramolecular 1D architectures.[11] We speculated that one type of novel D–A Intercalated-COFs could be built by the lateral growth of covalent layers via condensations of the D or A unit with suitable linkers and an synchronous vertical extension of the frameworks via supramolecular D–A interactions between the A or D unit and the covalent layer (Scheme 2). Notably, a few COFs involving D–A interactions have been reported albeit all with segregated D–A alignments because the electrostatic attractions for most D–A pairs are not strong enough to overcome the dispersion interactions between identical and large π-surfaces.[12] Therefore, stable alternating D–A stacking arrangements are an essential prerequisite for successful construction of a D–A Intercalated-COF. Herein, we employed electron-deficient and bulky 2,5,8,11-tetra(*p*-formylphenyl)-perylene diimide (PDI) **1** as an A unit, electron-rich perylene **3** with similar geometry as a D unit and also a guest, and *p*-phenylenediamine **2** as a linker. For **1** and **3**, strong homomeric interactions between identical π-surfaces that often lead to segregated D–A alignments are reduced due

Scheme 1. Schematic Illustration of Supramolecular Multicomponent 1D Stacks toward Intercalated-COF

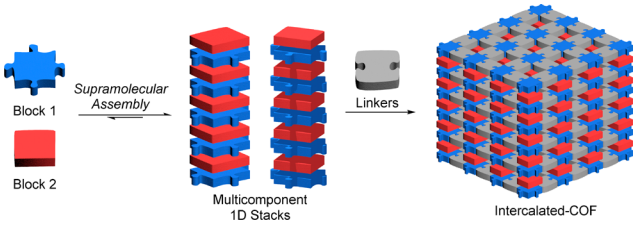

Received: December 23, 2019
Published: February 8, 2020

https://dx.doi.org/10.1021/jacs.9b13559
J. Am. Chem. Soc. 2020, 142, 3712–3717

Scheme 2. Schematic Representation of the Synthesis of (a) POP 4 in the Absence and (b) Intercalated-COF 5 in the Presence of D−A Interactions

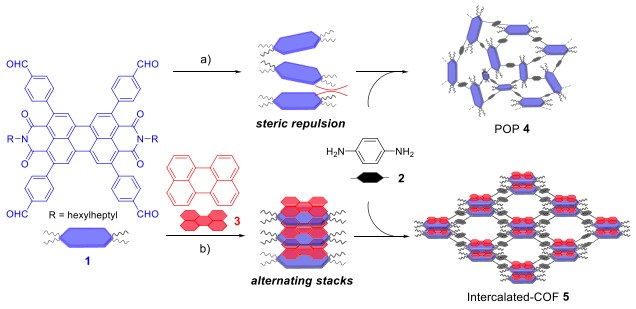

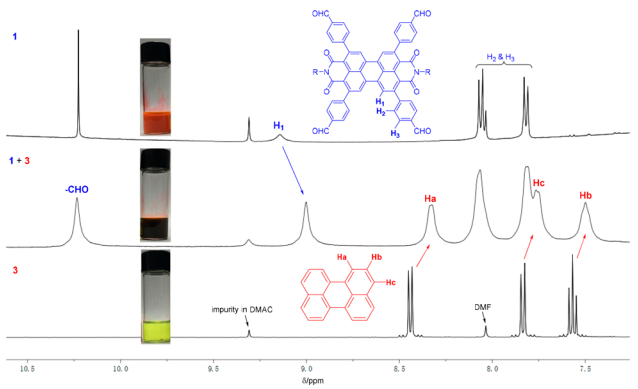

Figure 1. ^{1}H NMR spectra of **1**, **1**/ **3** (1:1), and **3** in 2:8 (v/v) DMF-d_7/DMAc and the actual color of **1**, the mixture, and **3**. (The concentrations of all components were kept at 5 mM.)

to the steric and electrostatic repulsions.[13] Instead, the stability of the alternating **1**−**3** stacks is significantly increased as the electrostatic attractions owing to large overlap of the π-surfaces and less pronounced steric crowding due to the buffering with planar molecule **3**.[14] Thus, **1** could polymerize with **2** in lateral directions and assemble with **3** into alternating D−A stacks along vertical directions to achieve the first Intercalated-COF, with alternating crystalline 2D ($(\mathbf{1}-\mathbf{2}_2)_n$: polymer having a 1:2 molar ratio of **1** to **2**) layers and intercalated guest (**3**) layers (Scheme 2b).

Based on our recent work,[15] *N*,*N*-bis(hexylheptyl)-2,5,8,11-tetra(*p*-formylphenyl)-PDI **1** with a flat perylene π-scaffold was synthesized readily (Scheme S1). The self-assembly behaviors of **1** in dimethylacetamide (DMAc) were thus investigated. The high value (1.5) of the A_{0-0}/A_{0-1} ratio of **1** in the UV/vis absorption spectra indicated that the stacking between the identical PDI rings is negligible in DMAc (Figure S1).[16] The solvothermal reactions of **1** with linker **2** were performed under vacuum at 120 °C in commonly used solvents such as DMAc, *n*-BuOH, dioxane/*ortho*-dichlorobenzene (*o*-DCB), DMAc/*o*-DCB, and *n*-BuOH/*o*-DCB. Due to the importance of $\pi-\pi$ stacking interactions for COF growth along vertical directions, these reactions only produce amorphous porous organic polymers (POP **4**) with no positive powder X-ray diffraction (PXRD) signals at small angles (Scheme 2a).

The D−A interactions between **1** and **3** were investigated by both ^{1}H NMR and UV−vis absorption spectroscopy. Upon mixing equimolar of **1** and **3** in the DMF-d_7/DMAc solution,[17] the aromatic protons of the perylene cores of both **1** and **3** shifted upfield with line broadening (Figure 1), indicating the formation of a strongly associating D−A complex and a fast equilibrium between the D−A complex and the individual components in solution.[18] In addition, the D−A interactions are clearly visible to the naked eye as upon mixing the DMAc solutions of **1** (red) and **3** (bright yellow) together, the color promptly changes to dark brown (Figure 1). At 20 °C, the 1:1 mixture of **1** and **3** in DMAc showed a broad absorption band centered at 680 nm, corresponding to the charge-transfer (CT) interactions between the D−A pair. Increasing the temperature up to 35 °C resulted in a progressive decrease of the CT band but with no peak shift, suggesting the disassembly of the CT complex (Figure S2).

Encouraged by these results, **1**, **3**, and **2** were employed to construct the first Intercalated-COF. To accelerate the imine formation between **1** and **2** while also maintaining the strong D−A interactions (<35 °C) between **1** and **3**, $Sc(OTf)_3$ was employed as the reaction catalyst.[19] After extensive optimizations, DMAc was found to be the optimal solvent. In a typical protocol, a 1:2:1 mixture of **1**, **2**, and **3** and 1 mL of DMAc in a 10 mL Pyrex tube was sonicated for 5 min at room temperature. To the stock solutions different amounts of $Sc(OTf)_3$ in DMAc were added. The combined solution was sonicated at room temperature for another 5 min and then kept at 30 °C for 3 days, after which the precipitate was collected by centrifugation, rinsed with solvents, and dried under vacuum to yield a red powder.[20] The PXRD patterns reveal reflections at 4.32°, 7.56°, and 8.40°, which are assignable to the (110), (210), and (220) facets of Intercalated-COF **5**, respectively. The presence of broader peaks corresponding to the (001) plane indicated the decrease in crystallinity along the *c* axis that can be attributed to the involvement of both the long alkyl chains[4b] and the intercalated perylene molecules between the COF layers (Figure 2A). Pawley refinements (dotted green curve) confirmed our peak assignments as evidenced by their negligible differences (black curves). The experimental PXRD patterns were in good agreement with the simulated patterns in AA-stacking, with perylene **3** as the guest molecule (orange curve). In stark contrast, the AA-stacking (magenta curve) and staggered AB-stacking (blue curve) mode of $(\mathbf{1}-\mathbf{2}_2)_n$ COF without guest intercalation could not reproduce the experimental XRD patterns. In particular, the presence of two peaks in the 2θ range of 4°−5° calculated for the traditional $(\mathbf{1}-\mathbf{2}_2)_n$ COF model further confirmed the formation of Intercalated-COF **5** (Figure 2).[21]

In the FT-IR spectra (Figure S3), the characteristic band of imine groups appears at 1620 cm^{-1} and dramatic attenuations of $-NH_2$ stretching vibrations and the C═O stretching vibration at 1698 cm^{-1} of **1** confirmed the successful formation of imine bonds. In addition, the peaks assigned to C−H out of plane bending vibrations of aromatic rings at 770 cm^{-1} in **5** is similar to that of the **1**−**3** CT complex, which further supports the D−A interactions in the 3D network. The CP/MAS ^{13}C NMR spectrum of **5** revealed the characteristic resonance peak of imine carbons at 158 ppm (Figure S4), further supporting the formation of imine bonds. The results of the elemental analysis of **5** were in good agreement with the expected chemical formulas (Table S1). Due to the existence of hydrocarbon **3**, Intercalated-COF **5** exhibited higher C and H content than **4**.

Thermogravimetry analysis (TGA) provided additional evidence (Figure 4a). The perylene molecule in the Intercalated-COF sample displayed a much higher sublimation

https://dx.doi.org/10.1021/jacs.9b13559
J. Am. Chem. Soc. 2020, 142, 3712−3717

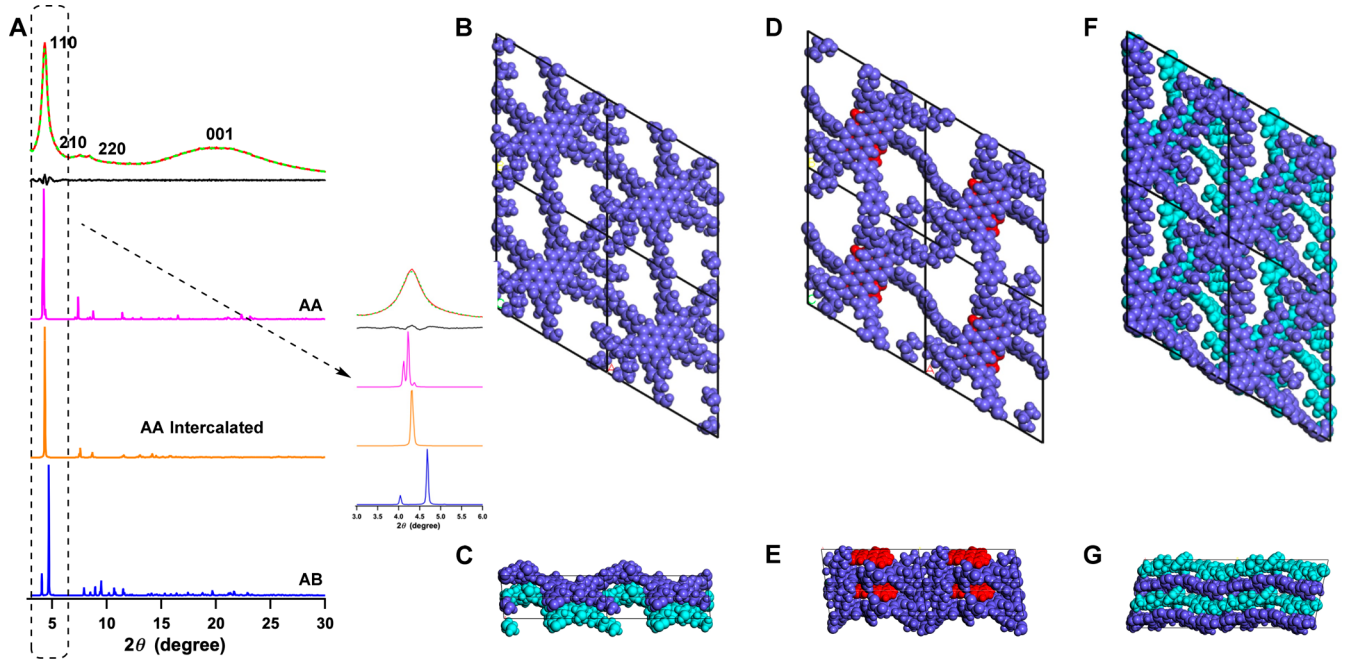

Figure 2. (A) Observed XRD patterns (red) and simulated profiles using the Pawley refinement (dotted green) of Intercalated-COF **5** and their difference (black), AA-stacking (magenta), AA-stacking with **3** as intercalation (orange), and staggered AB-stacking (blue) modes of the $(\mathbf{1}-\mathbf{2}_2)_n$ COF, respectively. (B, C) Unit cell structure of AA-stacking mode. (D, E) Unit cell structure of AA-stacking with **3** intercalation mode. (F, G) Unit cell structure of staggered AB-stacking mode.

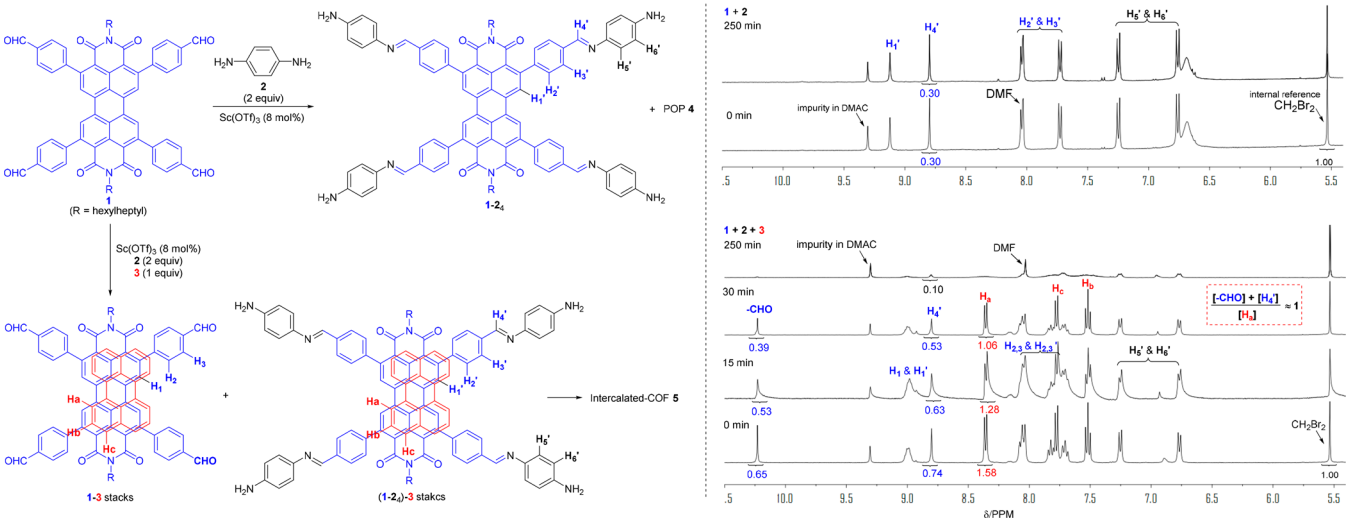

Figure 3. ^{1}H NMR spectra of a mixture of **1** (5 mM), **2** (10 mM), and Sc(OTf)$_3$ (1.6 mM) in the absence and in the presence of **3** (5 mM) in 2:8 (v/v) DMF-d_7/DMAc at 30 °C (CH_2Br_2: 1 mM).

temperature than that of both pure **3** and a 1:1 mixture of **1** and **3**, which indicates that the intercalated perylene is more stable during the test processes.[22]

Field emission scaning electron microscopy revealed that **5** displayed similar particle shapes with **4** but with a much larger size (Figure S5). The BET surface areas for **5** and **4** were determined to be 16 and 9 $m^2\ g^{-1}$, respectively (Figure S6). This result suggests that the inner space of **5** and **4** were fully occupied by the flexible swallow-tailed alkyl chains of **1**.[4b]

Monitoring the reaction course of **1** and **2** *in situ* in the absence or presence of perylene **3** may provide insight into the Intercalated-COF formation processes (Figure 3).[23] Addition of the catalyst Sc(OTf)$_3$ and 2 equiv of **2** in the solution of **1** immediately yields a precipitate. Besides the precipitation, NMR spectra of the solution indicated that the reactants **1** and **2** were quickly and completely consumed, leading to an imine product $(\mathbf{1}-\mathbf{2}_4)$ in solution. The precipitate was filtered and hydrolyzed with hydrochloric acid for NMR analysis (Figure S7), which suggested the formation of amorphous product $(\mathbf{1}-\mathbf{2}_2)_n$. In the presence of **3** (1 equal), the condensation between **1** and **2** becomes much slower probably because the aldehydes in the D−A stacks are more sterically hindered and less electron-deficient than the free ones.[24] Over a long period of time, two alternating D−A stacks **1**−**3** and $(\mathbf{1}-\mathbf{2}_4)-\mathbf{3}$ coexist in certain amounts in solution, and the ratio of **1** to **3** in these two stacks maintains at 1:1, indicating the ratio of **1** to **3** is also 1:1 in the crystallized Intercalated-COF.[25] As such, the D−A stacks have more time reorganizing into optimum conforma-

https://dx.doi.org/10.1021/jacs.9b13559
J. Am. Chem. Soc. 2020, 142, 3712−3717

tions to achieve high crystallinity. More importantly, the crystalline nature can provide the driving force for more stacks as growth units attaching to the crystal lattice and thus promote reactions until completion (Figure 3).

With this unique structure, diffuse reflectance UV−vis measurements of the solid state of these samples were carried out to extract reliable optical absorption profiles (Figure 4b).

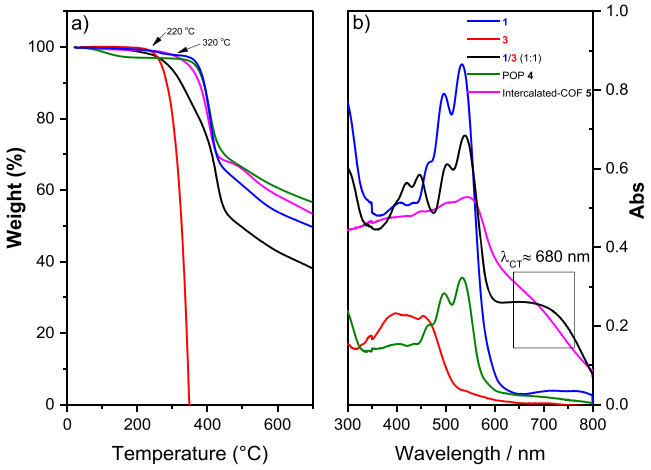

Figure 4. (a) TGA curves and (b) diffuse reflectance UV−vis absorption spectra of **1**, **3**, **1**/**3** (1:1), POP **4**, and Intercalated-COF **5**.

The A_{0-0}/A_{0-1} ratios of **1** (1.1) and POP **4** (1.1) suggested that there is no enhanced stacking between the PDI rings in **4**. On the contrary, for **5**, both broader PDI absorption maxima with a reduced A_{0-0}/A_{0-1} ratio and a new strong near-infrared-light absorption were observed (Figure 4b). With the CT band observed for the Intercalated-COF **5**, the fluorescence corresponding to PDI rings led to charge transfer induced quenching (Figure S8).[26]

In conclusion, based on a supramolecular strategy, we designed and constructed the first D−A type Intercalated-COF with alternating PDI-based covalent 2D layers and perylene guest layers. Strong homomeric interactions between identical π-surfaces that often lead to segregated D−A alignments are reduced here by employing sterically bulky 2,5,8,11-tetra(*p*-formylphenyl)-perylene diimide **1** and electron-rich perylene as the A and D unit, respectively. In situ monitoring of the reaction course by NMR indicated that the D−A stack formation is beneficial for the crystallization of the Intercalated-COF. Besides the chance for *z*-direction modulation of normal 2D-COFs, this supramolecular strategy also provides an atomically precise bottom-up approach toward well-defined robust heterostructures with diversified building blocks. We hope the innovative and unique Intercalated-COF structures could offer new nanotechnological applications, such as optoelectronic applications and exfoliation toward single layer COFs.

■ ASSOCIATED CONTENT

Supporting Information

The Supporting Information is available free of charge at https://pubs.acs.org/doi/10.1021/jacs.9b13559.

Synthesis and full characterization details of PDI **1**, POP **4**, and Intercalated-COF **5** (PDF)

■ AUTHOR INFORMATION

Corresponding Authors

Hui-Jun Zhang − *Department of Chemistry, College of Chemistry and Chemical Engineering, Xiamen University, Xiamen 361005, P. R. China;* orcid.org/0000-0001-9567-3010; Email: meghjzhang@xmu.edu.cn

Jianbin Lin − *Department of Chemistry, College of Chemistry and Chemical Engineering and MOE Key Laboratory of Spectrochemical Analysis and Instrumentation, Xiamen University, Xiamen 361005, P. R. China;* orcid.org/0000-0002-0064-3079; Email: jb.lin@xmu.edu.cn

Authors

Huiqing Li − *Department of Chemistry, College of Chemistry and Chemical Engineering, Xiamen University, Xiamen 361005, P. R. China*

Pengpeng Shao − *School of Chemistry and Chemical Engineering, Beijing Institute of Technology, Beijing 100081, P. R. China*

Shuqi Chen − *Department of Chemistry, College of Chemistry and Chemical Engineering, Xiamen University, Xiamen 361005, P. R. China*

Guosheng Li − *State Key Laboratory of Photocatalysis on Energy and Environment, and Key Laboratory of Molecular Synthesis and Function Discovery, College of Chemistry, Fuzhou University, Fuzhou 350116, P. R. China*

Xiao Feng − *School of Chemistry and Chemical Engineering, Beijing Institute of Technology, Beijing 100081, P. R. China;* orcid.org/0000-0002-3212-3051

Xiong Chen − *State Key Laboratory of Photocatalysis on Energy and Environment, and Key Laboratory of Molecular Synthesis and Function Discovery, College of Chemistry, Fuzhou University, Fuzhou 350116, P. R. China;* orcid.org/0000-0003-2878-7522

Yun-Bao Jiang − *Department of Chemistry, College of Chemistry and Chemical Engineering and MOE Key Laboratory of Spectrochemical Analysis and Instrumentation, Xiamen University, Xiamen 361005, P. R. China;* orcid.org/0000-0001-6912-8721

Complete contact information is available at: https://pubs.acs.org/10.1021/jacs.9b13559

Notes

The authors declare no competing financial interest.

■ ACKNOWLEDGMENTS

We are grateful for financial support from the Natural Science Foundation of China (Nos. 21772165, 21772162, 21572188), Natural Science Foundation of Fujian Province of China (2018J01014), Fundamental Research Funds for the Central Universities (No. 20720180031), and the Foundation for Innovative Research Groups of the National Natural Science Foundation of China (Grant No. 21521004).

■ REFERENCES

(1) (a) Feng, X.; Ding, X.; Jiang, D. Covalent organic frameworks. *Chem. Soc. Rev.* **2012**, *41* (18), 6010−6022. (b) Ding, S.-Y.; Wang, W. Covalent organic frameworks (COFs): from design to applications. *Chem. Soc. Rev.* **2013**, *42* (2), 548−568. (c) Waller, P. J.; Gándara, F.; Yaghi, O. M. Chemistry of Covalent Organic Frameworks. *Acc. Chem. Res.* **2015**, *48* (12), 3053−3063. (d) Huang, N.; Wang, P.; Jiang, D. Covalent organic frameworks: a materials platform for structural and functional designs. *Nat. Rev. Mater.* **2016**, *1*, 16068−16086.

(e) Diercks, C. S.; Yaghi, O. M. The atom, the molecule, and the covalent organic framework. *Science* **2017**, *355* (6328), eaal1585. (f) Jin, Y.; Hu, Y.; Zhang, W. Tessellated multiporous two-dimensional covalent organic frameworks. *Nat. Rev. Chem.* **2017**, *1* (7), No. s41570. (g) Beuerle, F.; Gole, B. Covalent Organic Frameworks and Cage Compounds: Design and Applications of Polymeric and Discrete Organic Scaffolds. *Angew. Chem., Int. Ed.* **2018**, *57* (18), 4850−4878. (h) Lohse, M. S.; Bein, T. Covalent Organic Frameworks: Structures, Synthesis, and Applications. *Adv. Funct. Mater.* **2018**, *28* (33), 1705553. (i) Chen, X.; Geng, K.; Liu, R.; Tan, K. T.; Gong, Y.; Li, Z.; Tao, S.; Jiang, Q.; Jiang, D. Covalent Organic Frameworks: Chemical Approaches to Designer Structures and Built-in Functions. *Angew. Chem., Int. Ed.* **2019**, *58*, DOI: 10.1002/anie.201904291.

(2) (a) Han, X.; Xia, Q.; Huang, J.; Liu, Y.; Tan, C.; Cui, Y. Chiral Covalent Organic Frameworks with High Chemical Stability for Heterogeneous Asymmetric Catalysis. *J. Am. Chem. Soc.* **2017**, *139* (25), 8693−8697. (b) Sick, T.; Hufnagel, A. G.; Kampmann, J.; Kondofersky, I.; Calik, M.; Rotter, J. M.; Evans, A.; Doblinger, M.; Herbert, S.; Peters, K.; Bohm, D.; Knochel, P.; Medina, D. D.; Fattakhova-Rohlfing, D.; Bein, T. Oriented Films of Conjugated 2D Covalent Organic Frameworks as Photocathodes for Water Splitting. *J. Am. Chem. Soc.* **2018**, *140* (6), 2085−2092.

(3) (a) Das, A.; Ghosh, S. Stimuli-Responsive Self-Assembly of a Naphthalene Diimide by Orthogonal Hydrogen Bonding and Its Coassembly with a Pyrene Derivative by a Pseudo-Intramolecular Charge-Transfer Interaction. *Angew. Chem., Int. Ed.* **2014**, *53* (4), 1092−1097. (b) Pramudya, Y.; Mendoza-Cortes, J. L. Design Principles for High H2 Storage Using Chelation of Abundant Transition Metals in Covalent Organic Frameworks for 0−700 bar at 298 K. *J. Am. Chem. Soc.* **2016**, *138* (46), 15204−15213.

(4) (a) Wang, S.; Wang, Q.; Shao, P.; Han, Y.; Gao, X.; Ma, L.; Yuan, S.; Ma, X.; Zhou, J.; Feng, X.; Wang, B. Exfoliation of Covalent Organic Frameworks into Few-Layer Redox-Active Nanosheets as Cathode Materials for Lithium-Ion Batteries. *J. Am. Chem. Soc.* **2017**, *139* (12), 4258−4261. (b) Zhang, G.; Hong, Y.-l.; Nishiyama, Y.; Bai, S.; Kitagawa, S.; Horike, S. Accumulation of Glassy Poly(ethylene oxide) Anchored in a Covalent Organic Framework as a Solid-State Li^+ Electrolyte. *J. Am. Chem. Soc.* **2019**, *141* (3), 1227−1234.

(5) (a) Lin, G.; Ding, H.; Yuan, D.; Wang, B.; Wang, C. A Pyrene-Based, Fluorescent Three-Dimensional Covalent Organic Framework. *J. Am. Chem. Soc.* **2016**, *138* (10), 3302−3305. (b) Zhu, M.-W.; Xu, S.-Q.; Wang, X.-Z.; Chen, Y.; Dai, L.; Zhao, X. The construction of fluorescent heteropore covalent organic frameworks and their applications in spectroscopic and visual detection of trinitrophenol with high selectivity and sensitivity. *Chem. Commun.* **2018**, *54* (18), 2308−2311.

(6) (a) Ma, H.; Liu, B.; Li, B.; Zhang, L.; Li, Y. G.; Tan, H. Q.; Zang, H. Y.; Zhu, G. Cationic Covalent Organic Frameworks: A Simple Platform of Anionic Exchange for Porosity Tuning and Proton Conduction. *J. Am. Chem. Soc.* **2016**, *138* (18), 5897−903. (b) Medina, D. D.; Sick, T.; Bein, T. Photoactive and Conducting Covalent Organic Frameworks. *Adv. Energy Mater.* **2017**, *7* (16), 1700387. (c) Xu, F.; Yang, S.; Chen, X.; Liu, Q.; Li, H.; Wang, H.; Wei, B.; Jiang, D. Energy-storage covalent organic frameworks: improving performance via engineering polysulfide chains on walls. *Chem. Sci.* **2019**, *10* (23), 6001−6006.

(7) (a) Smith, B. J.; Dichtel, W. R. Mechanistic Studies of Two-Dimensional Covalent Organic Frameworks Rapidly Polymerized from Initially Homogenous Conditions. *J. Am. Chem. Soc.* **2014**, *136* (24), 8783−8789. (b) Li, H.; Chavez, A. D.; Li, H.; Li, H.; Dichtel, W. R.; Bredas, J. L. Nucleation and Growth of Covalent Organic Frameworks from Solution: The Example of COF-5. *J. Am. Chem. Soc.* **2017**, *139* (45), 16310−16318.

(8) (a) Lukose, B.; Kuc, A.; Heine, T. The structure of layered covalent-organic frameworks. *Chem. - Eur. J.* **2011**, *17* (8), 2388−92. (b) Haase, F.; Gottschling, K.; Stegbauer, L.; Germann, L. S.; Gutzler, R.; Duppel, V.; Vyas, V. S.; Kern, K.; Dinnebier, R. E.; Lotsch, B. V. Tuning the stacking behaviour of a 2D covalent organic framework through non-covalent interactions. *Mater. Chem. Front.* **2017**, *1* (7), 1354−1361.

(9) (a) Chen, X.; Addicoat, M.; Irle, S.; Nagai, A.; Jiang, D. L. Control of Crystallinity and Porosity of Covalent Organic Frameworks by Managing Interlayer Interactions Based on Self-Complementary π-Electronic Force. *J. Am. Chem. Soc.* **2013**, *135* (2), 546−549. (b) Salonen, L. M.; Medina, D. D.; Carbo-Argibay, E.; Goesten, M. G.; Mafra, L.; Guldris, N.; Rotter, J. M.; Stroppa, D. G.; Rodriguez-Abreu, C. A supramolecular strategy based on molecular dipole moments for high-quality covalent organic frameworks. *Chem. Commun.* **2016**, *52* (51), 7986−9. (c) Auras, F.; Ascherl, L.; Hakimioun, A. H.; Margraf, J. T.; Hanusch, F. C.; Reuter, S.; Bessinger, D.; Doblinger, M.; Hettstedt, C.; Karaghiosoff, K.; Herbert, S.; Knochel, P.; Clark, T.; Bein, T. Synchronized Offset Stacking: A Concept for Growing Large-Domain and Highly Crystalline 2D Covalent Organic Frameworks. *J. Am. Chem. Soc.* **2016**, *138* (51), 16703−16710. (d) Ascherl, L.; Sick, T.; Margraf, J. T.; Lapidus, S. H.; Calik, M.; Hettstedt, C.; Karaghiosoff, K.; Doblinger, M.; Clark, T.; Chapman, K. W.; Auras, F.; Bein, T. Molecular docking sites designed for the generation of highly crystalline covalent organic frameworks. *Nat. Chem.* **2016**, *8* (4), 310−316. (e) Wu, X.; Han, X.; Liu, Y.; Liu, Y.; Cui, Y. Control Interlayer Stacking and Chemical Stability of Two-Dimensional Covalent Organic Frameworks via Steric Tuning. *J. Am. Chem. Soc.* **2018**, *140* (47), 16124−16133.

(10) Geim, A. K.; Grigorieva, I. V. Van der Waals heterostructures. *Nature* **2013**, *499*, 419.

(11) (a) Kumar, M.; Venkata Rao, K.; George, S. J. Supramolecular charge transfer nanostructures. *Phys. Chem. Chem. Phys.* **2014**, *16* (4), 1300−1313. (b) Das, A.; Ghosh, S. Supramolecular Assemblies by Charge-Transfer Interactions between Donor and Acceptor Chromophores. *Angew. Chem., Int. Ed.* **2014**, *53* (8), 2038−2054. (c) Zhang, J.; Xu, W.; Sheng, P.; Zhao, G.; Zhu, D. Organic Donor−Acceptor Complexes as Novel Organic Semiconductors. *Acc. Chem. Res.* **2017**, *50* (7), 1654−1662. (d) Jiang, H.; Hu, P.; Ye, J.; Zhang, K. K.; Long, Y.; Hu, W.; Kloc, C. Tuning of the degree of charge transfer and the electronic properties in organic binary compounds by crystal engineering: a perspective. *J. Mater. Chem. C* **2018**, *6* (8), 1884−1902. (e) Han, Y.; Tian, Y.; Li, Z.; Wang, F. Donor−acceptor-type supramolecular polymers on the basis of preorganized molecular tweezers/guest complexation. *Chem. Soc. Rev.* **2018**, *47* (14), 5165−5176.

(12) (a) Feng, X.; Chen, L.; Honsho, Y.; Saengsawang, O.; Liu, L.; Wang, L.; Saeki, A.; Irle, S.; Seki, S.; Dong, Y.; Jiang, D. An Ambipolar Conducting Covalent Organic Framework with Self-Sorted and Periodic Electron Donor-Acceptor Ordering. *Adv. Mater.* **2012**, *24* (22), 3026−3031. (b) Jin, S.; Furukawa, K.; Addicoat, M.; Chen, L.; Takahashi, S.; Irle, S.; Nakamura, T.; Jiang, D. Large pore donor-acceptor covalent organic frameworks. *Chem. Sci.* **2013**, *4* (12), 4505−4511. (c) Jin, S.; Ding, X.; Feng, X.; Supur, M.; Furukawa, K.; Takahashi, S.; Addicoat, M.; El-Khouly, M. E.; Nakamura, T.; Irle, S.; Fukuzumi, S.; Nagai, A.; Jiang, D. Charge Dynamics in A Donor−Acceptor Covalent Organic Framework with Periodically Ordered Bicontinuous Heterojunctions. *Angew. Chem., Int. Ed.* **2013**, *52* (7), 2017−2021. (d) Jin, S.; Supur, M.; Addicoat, M.; Furukawa, K.; Chen, L.; Nakamura, T.; Fukuzumi, S.; Irle, S.; Jiang, D. Creation of Superheterojunction Polymers via Direct Polycondensation: Segregated and Bicontinuous Donor−Acceptor π-Columnar Arrays in Covalent Organic Frameworks for Long-Lived Charge Separation. *J. Am. Chem. Soc.* **2015**, *137* (24), 7817−7827.

(13) Balakrishnan, K.; Datar, A.; Naddo, T.; Huang, J.; Oitker, R.; Yen, M.; Zhao, J.; Zang, L. Effect of Side-Chain Substituents on Self-Assembly of Perylene Diimide Molecules: Morphology Control. *J. Am. Chem. Soc.* **2006**, *128* (22), 7390−7398.

(14) Chakraborty, S.; Kar, H.; Sikder, A.; Ghosh, S. Steric ploy for alternating donor−acceptor co-assembly and cooperative supramolecular polymerization. *Chem. Sci.* **2017**, *8* (2), 1040−1045.

(15) (a) Zhang, L.; He, D.; Liu, Y.; Wang, K.; Guo, Z.; Lin, J.; Zhang, H.-J. 2,5,8,11-Tetraalkenyl Perylene Bisimides: Direct Regioselective Synthesis and Enhanced $\pi-\pi$ Stacking Interaction.

https://dx.doi.org/10.1021/jacs.9b13559
J. Am. Chem. Soc. 2020, 142, 3712−3717

Org. Lett. **2016**, *18* (22), 5908−5911. (b) Wu, J.; He, D.; Zhang, L.; Liu, Y.; Mo, X.; Lin, J.; Zhang, H.-J. Direct Synthesis of Large-Scale *Ortho*-Iodinated Perylene Diimides: Key Precursors for Functional Dyes. *Org. Lett.* **2017**, *19* (19), 5438−5441. (c) Wu, J.; He, D.; Wang, Y.; Su, F.; Guo, Z.; Lin, J.; Zhang, H.-J. Selective Ortho-π-Extension of Perylene Diimides for Rylene Dyes. *Org. Lett.* **2018**, *20* (19), 6117−6120. (d) Su, F.; Chen, G.; Korevaar, P. A.; Pan, F.; Liu, H.; Guo, Z.; Schenning, A.; Zhang, H.-J.; Lin, J.; Jiang, Y. B. Discrete π-Stacks from Self-Assembled Perylenediimide Analogues. *Angew. Chem., Int. Ed.* **2019**, *58* (43), 15273−15277.

(16) Spenst, P.; Young, R. M.; Phelan, B. T.; Keller, M.; Dostál, J.; Brixner, T.; Wasielewski, M. R.; Würthner, F. Solvent-Templated Folding of Perylene Bisimide Macrocycles into Coiled Double-String Ropes with Solvent-Sensitive Optical Signatures. *J. Am. Chem. Soc.* **2017**, *139* (5), 2014−2021.

(17) 2:8 (v/v) DMF-d_7/DMAc were mixed to keep the resonance frequency constant.

(18) Klivansky, L. M.; Hanifi, D.; Koshkakaryan, G.; Holycross, D. R.; Gorski, E. K.; Wu, Q.; Chai, M.; Liu, Y. A complementary disk-shaped π electron donor−acceptor pair with high binding affinity. *Chem. Sci.* **2012**, *3* (6), 2009−2014.

(19) (a) Giuseppone, N.; Schmitt, J. L.; Schwartz, E.; Lehn, J. M. Scandium(III) Catalysis of Transimination Reactions. Independent and Constitutionally Coupled Reversible Processes. *J. Am. Chem. Soc.* **2005**, *127* (15), 5528−5539. (b) Matsumoto, M.; Dasari, R. R.; Ji, W.; Feriante, C. H.; Parker, T. C.; Marder, S. R.; Dichtel, W. R. Rapid, Low Temperature Formation of Imine-Linked Covalent Organic Frameworks Catalyzed by Metal Triflates. *J. Am. Chem. Soc.* **2017**, *139* (14), 4999−5002.

(20) Little to no precipitation was observed from reactions without catalyst. In contrast, PXRD patterns of solids formed in the presence of 0.04−0.12 equiv of $Sc(OTf)_3$ relative to the aldehyde groups show sharp diffraction peaks and 0.08 equiv has the highest intensity in the presence of **3**.

(21) Control experiments showed that **1** and **2** with catalyst without CT interaction (in the absence of perylene **3** or in the presence of **3** at 120 °C) only provided **4**.

(22) Although the perylene molecules in a 1:1 mixture of **1** and **3** displayed the same decomposition temperature as that of pure **3**, the sublimation rate is much slower because of the equilibrium between individual components and the D−A stacks. See: Zhang, D. S.; Gao, Q.; Chang, Z.; Liu, X. T.; Zhao, B.; Xuan, Z. H.; Hu, T. L.; Zhang, Y. H.; Zhu, J.; Bu, X. H. Rational construction of highly tunable donor-acceptor materials based on a crystalline host-guest platform. *Adv. Mater.* **2018**, *30*, No. 1804715.

(23) **1** alone and the 1:1 mixture of **1** and **3** were both initially heated in DMF-d_7/DMAc for a few minutes to fully dissolve, which can remain in solution upon cooling to 30 °C. Due to the low concentration of **1** and **3** in the solution of (**1** + **2** + **3**), most of **1** and **3** were in dissociated monomer state in solution and therefore showed ^{1}H NMR spectra with sharp peaks.

(24) Neel, A. J.; Hilton, M. J.; Sigman, M. S.; Toste, F. D. Exploiting non-covalent π-interactions for catalyst design. *Nature* **2017**, *543*, 637−646.

(25) The intercalated-COF **5** was also etched with hydrochloric acid. However, the molar ratio of **3** to **1** is less than 1 probably due to **3** on the surface of the materials is easily washed away during postprocessing.

(26) Spenst, P.; Würthner, F. A Perylene Bisimide Cyclophane as a "Turn-On" and "Turn-Off" Fluorescence Probe. *Angew. Chem., Int. Ed.* **2015**, *54* (35), 10165−10168.

https://dx.doi.org/10.1021/jacs.9b13559
J. Am. Chem. Soc. 2020, 142, 3712−3717